ISSN 0354-8724 (hard copy) | ISSN 1820-7138 (online)

# River Ice Monitoring of the Danube and Tisza Rivers using Sentinel-1 Radar Data

**Boudewijn van Leeuwen[A*], György Sipos[A], Jenő Lábdy[B], Márta Baksa[B], Zalán Tobak[A]**

Received: August 04, 2022 | Revised: September 21, 2022 | Accepted: September 21, 2022
doi: 10.5937/gp26-39962

***Abstract***

Due to extreme weather, occasionally Hungary's main rivers and lakes grow an ice cover causing severe damage to infrastructure and increased flood hazard. During cold periods in 2017 and 2022, a dangerous layer of ice developed on the main rivers in the country. Since river ice is rare in this region, no permanent ice monitoring system is in operation. Due to their all weather capabilities, active remote sensing instruments provide a good opportunity to monitor ice coverage. ESA's Sentinel-1 radar satellites acquire data with a relatively high spatial and temporal resolution. A method was developed to provide ice coverage information at a regular interval; depending on the satellite revisit, at least once every 5 days, but often also on a daily basis. In 2017, maps were created for sections along the Danube and in 2022 for another section of the Tisza river. The ice coverage was calculated with a spatial resolution of 10 metre and visualised with a spatial density of 100 metre along the rivers. The mapping procedure provides visual information to give a fast overview of the spatial extent of ice coverage and quantitative, tabular information for operational activities to mitigate the damage due to ice packs and ice jams.

**Keywords:** river ice; classification; Sentinel-1; flood; radar; Danube; Tisza

## Introduction

January 2017 was the coldest month in Hungary in 30 years. The extreme temperatures were due to a Canadian High and Siberian anticyclone resulting in a large stationary high pressure area over Europe which caused cold air to flow from Scandinavia and Russia to Central and Eastern Europe (Horváth, 2017). The average daily temperature in Hungary in January was -5.8 °C, which is 4.5 °C lower than the long term annual mean. Due to a thin layer of snow and clear skies, the temperature dropped to its lowest point of -28.1 °C in Tésa on January 8. After a short, slightly warmer period in the middle of the month, a new, extremely cold period followed with average daily temperatures well below -6 °C (OMSZ, 2017). Due to the continuous low temperatures, ice developed on Hungary's main rivers and lakes (Gombás & Balatonyi, 2017; Liptay et al., 2021). From January 6 until February 3, 2017, everywhere along the Danube large patches and packs of river ice occurred (Takács & Kern, 2017). Although in the winter season of 2021/2022, the average monthly temperatures were not extreme (2.3 and 1.1°C in December and January at Szeged), there was a long cold period with average daily temperatures below 0°C from January 7 till January 25, 2022. (https://ogimet.com). The daily maximums were between 0-5°C, but the daily minimums were below freezing point, sometimes even below -10°C. These meteorological conditions resulted in river ice development on Tisza River.

The presence and frequency of floating or static ice on the largest rivers in the Carpathian Basin has changed a lot in the last 120 years (Takács et al., 2018; Keve, 2017b). While earlier floods caused by ice were

[A] Department of Geoinformatics, Physical and Environmental Geography, University of Szeged, 6722 Szeged, Egyetem str. 2-6. leeuwen@geo.u-szeged.hu; gysipos@geo.u-szeged.hu; tobak@geo.u-szeged.hu
[B] General Directorate of Water Management, 1012 Budapest, Márvány utca 1/d. labdy.jeno@ovf.hu; baksa.marta@ovf.hu
[*] Corresponding author: Boudewijn van Leeuwen; e-mail: leeuwen@geo.u-szeged.hu

a common phenomenon (at the Danube in 1838, 1839, 1850, 1876, 1878, 1883, 1891, 1920, 1923, 1926, 1929, 1940, 1941 and 1956, Keve, 2017b), from the second half of the 20th century, static ice cover occurred only sporadically (e.g. in 1962/1963 for a longer period and last time in 1984/1985, Takács & Kern, 2017). From 2000 not just static ice formation but also the occurrence and duration of ice floe periods decreased (Ionita et al., 2018). Since 2000, the ice floe period has never been longer than 20 days. Floating ice could be observed along the Danube (Budapest and Mohács) for more than 10 days in 2005/2006, 2011/2012 and 2016/2017 (Takács & Kern, 2017).

The development of river ice increases the risk of flooding, damage to infrastructure and transportation problems (Highs, 2009; Chu et al., 2015; Agafonova et al., 2017). The high pressure of the ice can cause problems in harbours, docks, buildings, and other flood defence structures. It can also damage the river bank and its vegetation. In Hungary, in addition to local protection measures, an icebreaker fleet is being deployed to combat river ice (Gombás & Balatonyi, 2017). Icebreakers are used to make rivers accessible for transport and reduce the pressure on infrastructure caused by ice collisions. It is important to map the ice coverage to optimize protection measures. However, as river ice does not occur often, no permanent monitoring system, covering the main rivers, is installed like in other countries with regular occurrence of river ice (Keve, 2014). The only attempt to monitor river ice in Hungary known to the authors is a network of five web cameras (four cameras, of which three on the Danube and one on the Tisza, were still operational in March 2022) on a 130 kilometer long segment of the Danube (Keve, 2017a). Permanent monitoring systems are expensive to maintain, restricted to a limited number of places and are technically challenging (Keve, 2017b; Keve 2020).

Active remote sensing data can be acquired at relatively fine spatial resolutions and operate in the microwave range. This circumvents the effect of haze and cloud cover and provides potential opportunities for the development of valuable automatic and periodic river-ice monitoring tools (Chu et al., 2015). Since 2015, ESA's Sentinel-1 radar satellites acquire data with a high spatial and high temporal resolution (Malenovský et al., 2012). This data provides new possibilities for the semi-permanent monitoring of ice coverage of large rivers and lakes (Van Leeuwen et al., 2018). Earlier research demonstrated that remote sensing data can be used to detect, classify and monitor ice on sea or on large lakes (Tom et al., 2020; Howell et al., 2021; Zhang et al., 2021; Lohse et al., 2020; Li et al., 2021). River ice monitoring in Arctic regions has been conducted by several authors: Weber et al. (2003) used active data, Altena et al. (2021) applied different optical data sets, Goldberg et al. (2020) worked with low resolution RS data to predict ice jams, and Zakharova et al. (2021) used altimetry to classify river ice. Our research is the first attempt to monitor river ice coverage in a continental climate using high resolution radar data. Our aim is to monitor the development of ice cover on the Danube and Tisza rivers in Hungary. Here, we present the validation, improvements and spatial extension of the algorithm introduced in our preliminary research on the Danube (Van Leeuwen et al., 2018). Other characteristics like thickness, chemical composition and typisation of the ice were not the scope of this research.

## Data and methods

### Study area

The study areas for this research cover a major part of the Middle Danube in the Carpathian Basin where most river ice is formed. The Danube study area stretches from Dunaföldvár in Hungary, via Croatia to Belgrade in Serbia. The Lower Tisza River study area extends from Algyő in Hungary to Kanjiza in Serbia (Figure 1). This section of the Tisza was selected because of the extend of ice coverage in 2022 and it was operationally easy to validate the ice detection methods at this location. The Danube is a major river in Europe with a mean discharge of 2350 $m^3/s$ at Budapest and 5600 $m^3/s$ at Belgrade (Mezősi, 2016). The Middle Danube is an alluvial river on the investigated reach and has a meandering pattern in general. However, numerous bends were cut-off artificially during the regulation works of the 19$^{th}$ century (Somogyi, 2001), and the originally ~540 km long reach was reduced to 400 km. The most affected sections were located between Paks and Baja, and between Mohács and Apatin (Fig. 1). A major motivation behind river training at that time was to prevent so called ice jam floods, developing by the ramping of ice floes at riffles and in meanders, which blocked river flow and caused serious upstream impoundment. Flood hazard was boosted by meteorological reasons as well, since general thawing advances from west to east in the region; thus, meltwater flood waves increased both ice ramping and inundation. Nevertheless, meander cut-offs just partly solved the problem, as the river channel is still shallow and wide, several islands exist, and riffles do also develop.

The Tisza is the second largest river in the Carpathian Basin and the largest tributary of the Danube. The

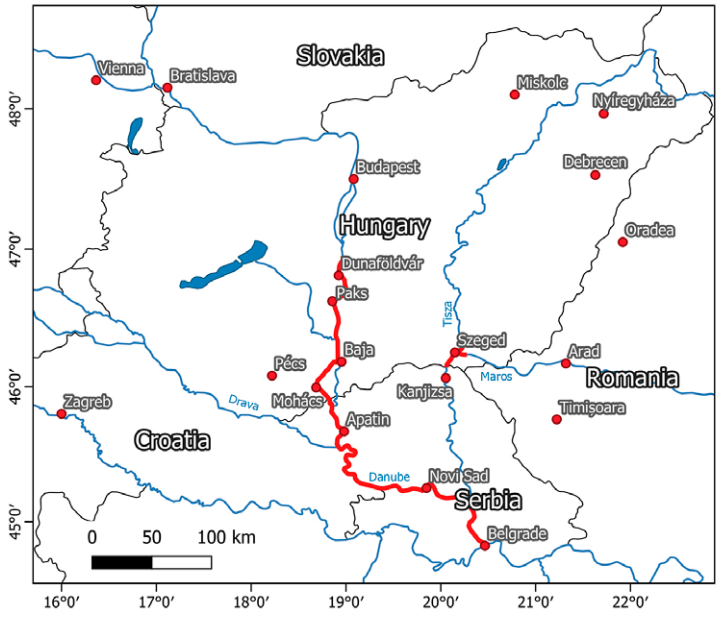


**Figure 1.** Study areas along the Danube and Tisza/Maros river

river is strongly regulated, i.e. its channel was shortened radically, by almost 40 % (Somogyi, 2001). Its mean discharge is 825 m³/s at Szeged (Kiss et al., 2019). The Tisza is less frequently endangered by ice jam floods. This is partly because on its catchment general spring thaw advances from southwest to northeast, i.e. opposite to its flow direction, and partly because the width/depth ratio of its channel is significantly lower than that of the Danube. The analysed river section is 40 km long and located at the Hungarian-Serbian border. The study area contains a short section of the Maros, which is the largest tributary of the Tisza.

## Data

The identification of ice on the rivers is based on radar data from the Sentinel-1A and Sentinel-1B satellites. The satellites are equipped with identical 5.405 GHz C-band Synthetic Aperture Radar (SAR) instruments. In the presented workflow, we are using the Level-1 Ground Range Detected (GRD) product. Data is collected in the Interferometric Wide (IW) swath mode and has a 250 km swath width and a pixel spacing of 10 x 10 metre (Malenovský et al., 2012). The data product comes with VV and VH polarisation over land masses, but only the VV polarisation was used in our research. Data for the period from 1 January to 15 February 2017 and 19 January to 29 January 2022 was downloaded from Copernicus Open Access Hub. The data is free of charge and without restrictions of use.

The Sentinel-1 satellites form a constellation that provides an image of the area under investigation about every third day. The study areas are covered by three ascending and two descending paths, so the river sections are never covered by just one image; for each day, it is needed to mosaic different images. Since radar data is more or less independent from weather circumstances, atmospheric conditions do not disturb the data acquisition and every image that is acquired by the satellites can be used for information extraction. Unfortunately, due to a major anomaly, Sentinel-1B does not provide data since 23 December 2021, and only data from Sentinel-1A was used during the cold period in 2022.

## Software

All preprocessing is carried out in ESA's SNAP open-source image processing software. Further processing and mapping are executed in ArcGIS Desktop. The processing is automated with a graph in SNAP and Python scripting in ArcGIS.

## Data processing

### *Data preprocessing*

To be able to extract useful information from the radar images, the raw radar GRD IW data need to be geometrically corrected and radiometrically calibrated. The process is presented in Figure 2. After downloading the image, the orbit state vector available from the metadata can be automatically updated, if a precise orbit file is available. In the next step, the image is calibrated to convert the raw pixel values to unbiased backscatter values. To reduce noise, which is inherent to radar images, a single image speckle filter is applied. The image is then geometrically corrected using the object-sensor geometry and a digital elevation mod-

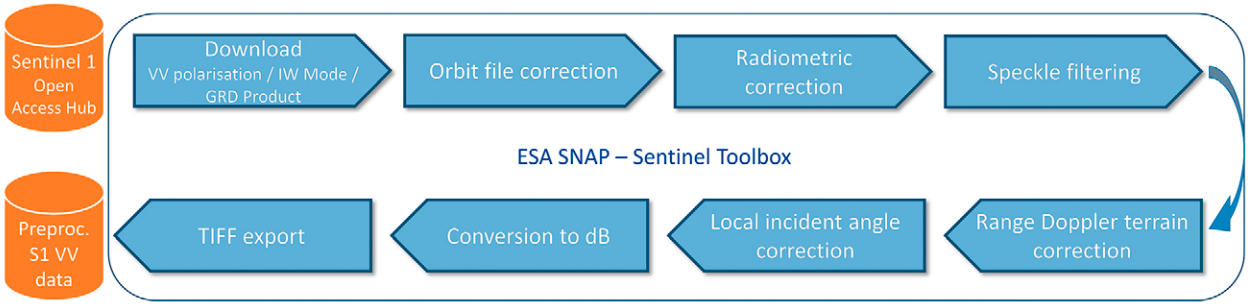


**Figure 2.** Raw data processing in ESA SNAP

el. In this step, also a map is created that stores the local incidence angle for each pixel in the image. Using this map, the backscatter values are normalised. Finally, the backscatter values are converted to decibel and stored as a GeoTIFF file for further processing in a geographic information system.

### *Creation of river polygons*

The base data for the river polygon files was a 1:50,000 vector file acquired from the Hungarian General Directorate of Water Management. The file was clipped to both study areas. The resulting files for the Danube and Tisza areas were then draped over very high resolution GeoEye imagery in Google Earth and manually edited to reduce errors due to shadows, sandbanks, islands, and man-made structures. For both rivers, the centreline was extracted and perpendicular intersections with a spacing of 100 metre were calculated. For the Danube, the 405 km long polygon was split along its centreline into 4050 one-hundred-metre sections. The Tisza polygon map resulted in an approximately 40 km long polygon, with 371 one hundred metre sections along the Tisza and Maros. In both polygon files, islands, meanders, splittings and other problems were manually corrected, and the sectors were adjusted manually to coincide with the fluvial kilometre (fkm) markings of the Hungarian water directorate.

### *Ice detection*

The strength of backscattered radar signals is highly dependent on the dielectric properties of the surface. The dielectric constant of clear and dry ice is between 2.0 and 3.2, while the dielectric constant of water is 80. Therefore, water results in a lower signal than dry ice. Ice with a rough surface gives the highest signal, while smooth non turbid water gives the lowest signal (Figure 3). A thawing ice layer with a higher dielectric constant and higher water and moisture content, produces a higher return signal compared to that of the layers with low dielectric constant, such as clear and dry snow/ice layers (Chu et al., 2015). The variation in ice roughness, water content and smoothness of the water makes it challenging to determine the boundary between water and ice.

After normalisation of the local incidence angle, the backscattered radar signal consists of two components: 1) surface scattering and 2) volume scattering. Smooth surfaces result in lower surface scattering, because the incoming radar signal is reflected away from the sensor, while rough surfaces have a higher signal due to diffuse surface scattering. Volume scattering is higher for ice surfaces with lots of cracks and impurities (Chu et al., 2015).

In this study, based on visual identification of the ice cover, we defined a threshold that - within the area of the river - separates surfaces below the threshold as water and above the threshold as ice (Figure 4). In this way, a binary raster map with ice and no ice pixels can be created. This raster is then converted to a polygon file and intersected with the river polygon file. For each of the 100 metre sections of the fkm file, the ratio between water and ice was calculated.

### *Mapping*

The main goal of the mapping workflow was to create printed layouts with all information necessary for the operative decision making process. The image processing steps were conducted on individual satellite scenes.

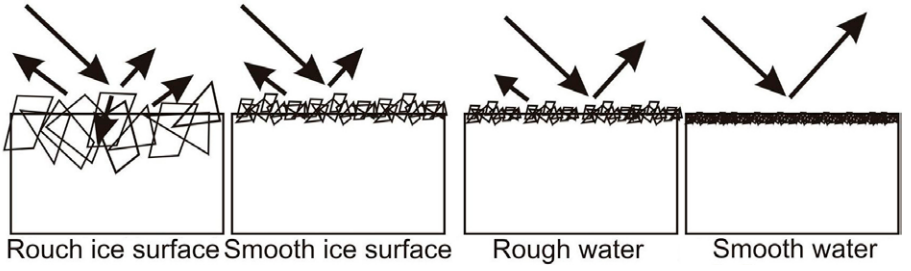


**Figure 3.** Relationship between ice surface and strength of the backscatter signal (Based on Unterschultz et al., 2009)

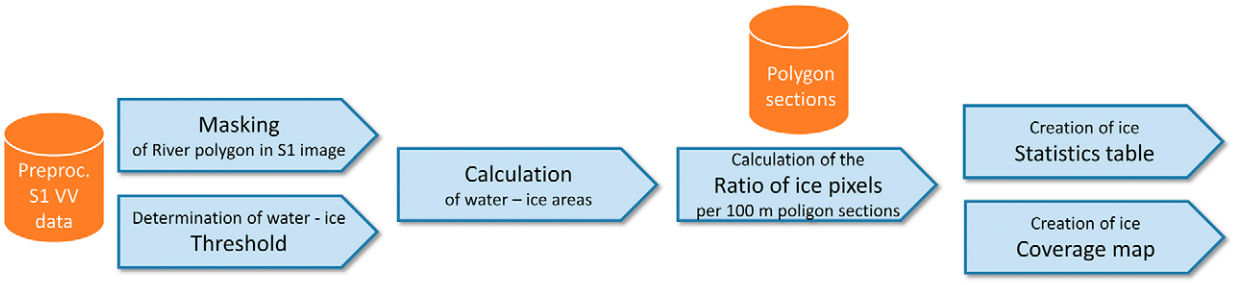


**Figure 4.** Processing workflow for determining ice cover from preprocessed satellite images

Therefore, the calculated ice cover maps of the same satellite path were merged, and the overlapping areas of ascending and descending satellite paths were mosaiced. The continuous ice cover dataset was aggregated into polygons covering 100 metre sections along the river. In this way, not only the actual position, but also the proportion of the ice cover is visualised.

Printable layouts were generated for each day when satellite data was available of the study area. In the case of the Danube, the whole 400 km section was divided into 8 smaller parts. This way the layouts could have better resolution when printed on A3 paper format. They contain multiple map frames to visualise the calculated ratio of ice cover in 100 metres sections, and the exact location of the identified ice blocks as well. The layers' symbology was generated based on the advice of the Hungarian General Directorate of Water Management to provide easily interpretable information. Optionally, the layouts can contain alphanumeric information in tabular form, presenting the exact ice cover ratio values in 100 metres sections. The dynamics of the ice cover can be visualised using the layouts of a selected river section on different dates.

## Validation methods

There are no independent data sets that provide continuous information on the ice coverage of the Danube and Tisza, therefore quantitative validation of our results is problematic. Two methods have been applied to evaluate the quality of our methods. The first method is based on observations by inspectors of the Hungarian General Directorate of Water Management for the Danube River. The second method is based on comparison with independent data obtained from other optical satellites.

### *Comparison with ice watch data*

Daily observations of ice coverage by inspectors of the Hungarian General Directorate of Water Management are aggregated to maps and tabular data with a spatial resolution of about 1 kilometre between the 1850 and 1440 fkm (Rajka, Hungary - Mohács, Hungary). This information is published on the hydroinfo webpage of the Hungarian General Directorate of Water Management (http://www.hydroinfo.hu/). A section to the south of Dunaföldvár with a length of 5 kilometres was selected to be compared to the satellite-derived ice coverage. The hydroinfo data is published in five ordinal classes: No ice, small ice cover, medium ice cover, large ice cover, completely covered. The radar derived ice coverage in percentage was aggregated to the same section as the observation.

### *Comparison with multispectral imagery*

Multispectral data was evaluated as a source for validation of the presented method. Landsat 8 and Sentinel-2 data were considered, because they have similar resolution as Sentinel-1, they can be acquired free of charge and Sentinel-2 has a high temporal resolution. Landsat 8 and Sentinel-2 data are not acquired at the same time as Sentinel-1 data, but for the research, it was assumed that if data was acquired on the same day, the ice coverage should be comparable. Unfortunately, during the one and a half month long research period in 2017, only one usable Landsat 8 image was acquired on the same day as Sentinel-1. All other Landsat 8 or Sentinel-2 images were cloudy or collected on a different day. On January 22, 2017, a Landsat 8 image was acquired at 09:33 UTC, while a Sentinel-1 image was acquired at 16:33 UTC. The images overlap each other in a small area in Hungary. Obviously, the 7-hour difference between the image acquisitions limits the reliability of the validation. The validation at the Tisza in 2022 was conducted based on comparison between completely overlapping Sentinel-1 and Sentinel-2 images of the same day (January 24). The time difference was 5 hours. To evaluate the calculated ice cover map, the multispectral dataset was clustered into 15 classes using ISODATA algorithm and the corresponding classes were labelled as ice cover.

## Data analysis

Beside developing, testing and validating an ice monitoring algorithm, the data obtained from the 2017 Danube ice survey was analysed in order to assess the temporal and spatial pattern of ice formation, and to determine what factors most severely affect the development of static ice cover on the river.

For the analyses the tabular data of those days were used when satellite coverage was complete for the entire section. In all, 11 full coverages could be assessed (3rd, 9th, 15th, 16th, 22nd, 27th, 28th of January and 3rd, 8th, 9th, 15th of February). For these days, first a mean daily ice cover ratio was determined, then a distance based mean ice cover graph was made, showing representative ice cover values for each 100 m polygon for the entire period. Daily mean temperature data were derived from the meteorologic station of Hódmezővásárhely, Hungary, being approximately at the centre of the study area.

Beside temperature, icing is also determined by channel geometry, reach scale and local changes in flow conditions, and by obstacles in the channel (Lal & Shen, 1993). As flow conditions could not be reconstructed for the entire section, we mostly focused on planform channel geometry data. Accordingly, the spatial distribution of ice cover data was first compared to channel width, and channel width variation. Width values were derived from the 100 m river polygons. Width variation was determined by subtracting each width data from the consecutive downstream value. A more negative value meant a more significant narrowing along the section and vice versa. Channel roughness can also be increased by the presence of mid-channel islands, therefore, these were mapped and overlaid on the ice data as well. Ice coverage was also assessed in relation with river sinuosity, taken from the arc/chord length ratio of river bends. Arc length was determined along the channel centreline in between two inflection points, while the chord length was taken as the straight-line distance of the points. Finally, ice cover was also compared to water surface slope conditions of the investigated reach, calculated from the absolute height of gauge stations (Dunaföldvár, Paks, Baja, Dunaszekcső, Mohács, Apatin, Novi Sad, Pancevo) and flood free low water data. We chose this approach to be able to determine which channel sections have below and above average channel slope.

## Results and discussion

### Ice coverage maps

For the complete ice periods in 2017 and 2022, maps were generated showing the ice coverage per pixel (at the resolution of the satellite data) and aggregated to the 100 metre sections of the rivers. Figure 5 shows a 36 kilometre long example of the ice coverage detection algorithm. The results show coverage and ratio of coverage per 100 metre section. The series of coverage maps and the 100 m resolution coverage ratio data also allowed the identification of reaches mostly affected by the formation of complete ice cover and ice jams and the evaluation of ice formation in relation with changes in river morphology. In general, ice packing was detected mostly at sections with fluvial islands or with mature meanders. Figure 6 shows the same type of result for the Tisza section in 2022. Here, the ice formed a blockage upstream of a sharp bend east of Szeged. As a result, a 3.8-kilometre-long stretch of the river was almost completely covered with ice.

In total 173 layouts in A3 format, with a scale of 1:100,000 were produced to visualise the ice coverage

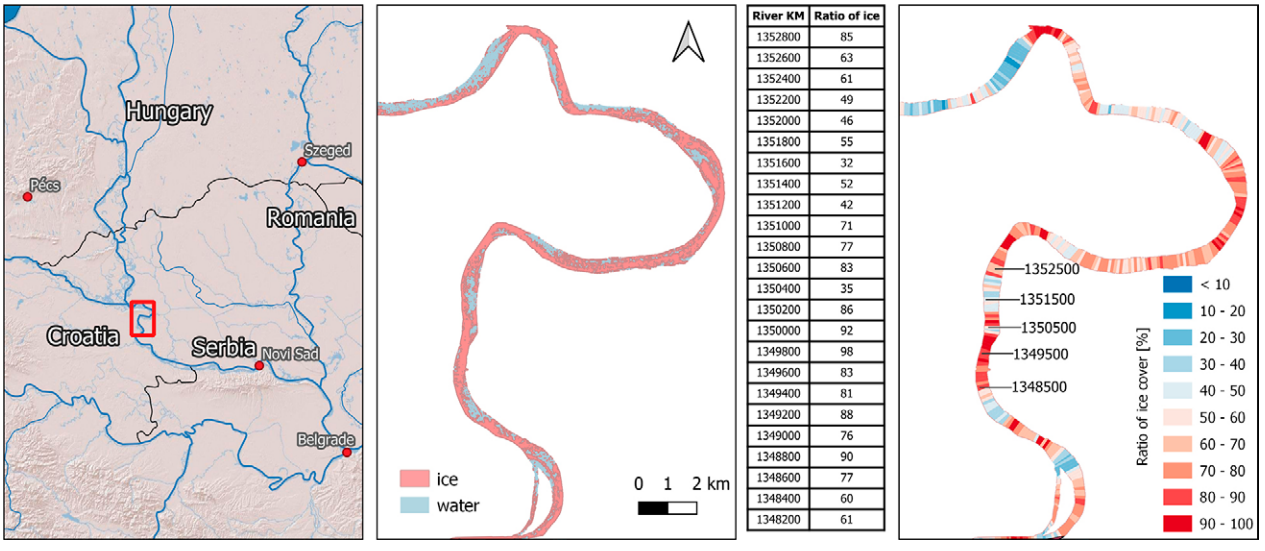


| River KM | Ratio of ice |
|---|---|
| 1352800 | 85 |
| 1352600 | 63 |
| 1352400 | 61 |
| 1352200 | 49 |
| 1352000 | 46 |
| 1351800 | 55 |
| 1351600 | 32 |
| 1351400 | 52 |
| 1351200 | 42 |
| 1351000 | 71 |
| 1350800 | 77 |
| 1350600 | 83 |
| 1350400 | 35 |
| 1350200 | 86 |
| 1350000 | 92 |
| 1349800 | 98 |
| 1349600 | 83 |
| 1349400 | 81 |
| 1349200 | 88 |
| 1349000 | 76 |
| 1348800 | 90 |
| 1348600 | 77 |
| 1348400 | 60 |
| 1348200 | 61 |

**Figure 5.** Results of the radar based ice coverage calculation of January 10, 2017 for a Danube river subsection in Croatia (left), the 10 x 10 metre resolution ice coverage (middle) and the polygon map showing the ratio of the river covered with ice per 100 metre section (right)

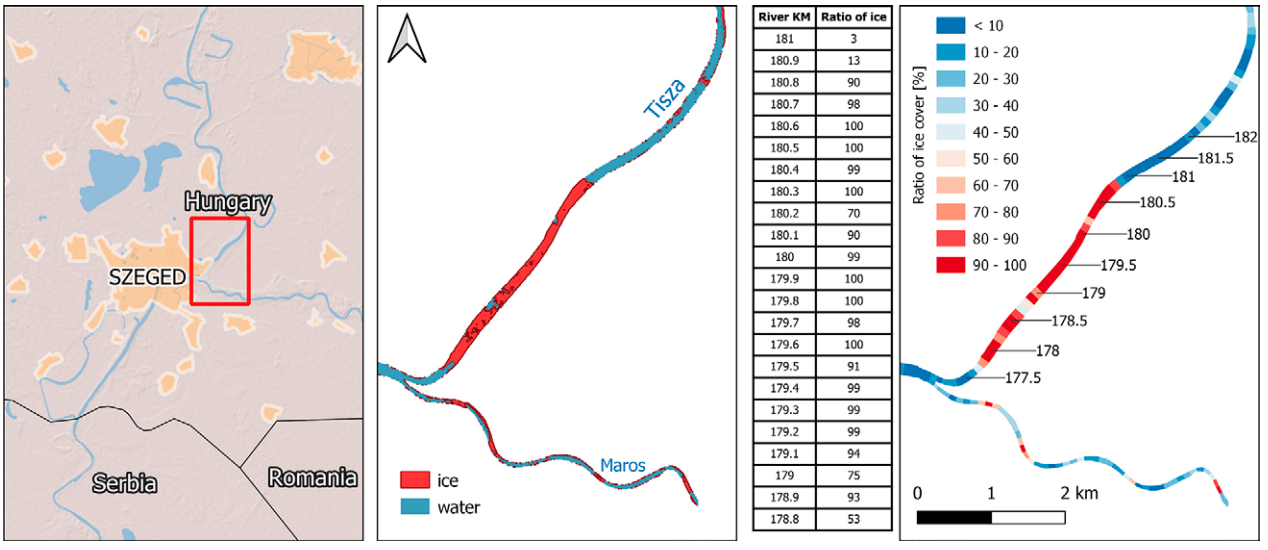


**Figure 6**. Results of the radar based ice coverage calculation of January 27, 2022 for a Tisza subsection near Szeged in Hungary (left), the 10 x 10 metre resolution ice coverage (middle) and the polygon map showing the ratio of the river covered with ice per 100 metre section (right)

on the Danube in 2017. Each layout shows a river section of around 50 km. The language of the layout is Hungarian because they are produced for operational activities of the Hungarian General Directorate of Water Management water management. An example of a printable map in Serbia is given in Figure 7.

## Validation of results

The Sentinel-1 derived ice coverage maps were compared to the in-situ observations by the Hungarian General Directorate of Water Management for the long ice period in 2017 (Figure 8). The ice coverage pattern shown by in-situ observations is an in-

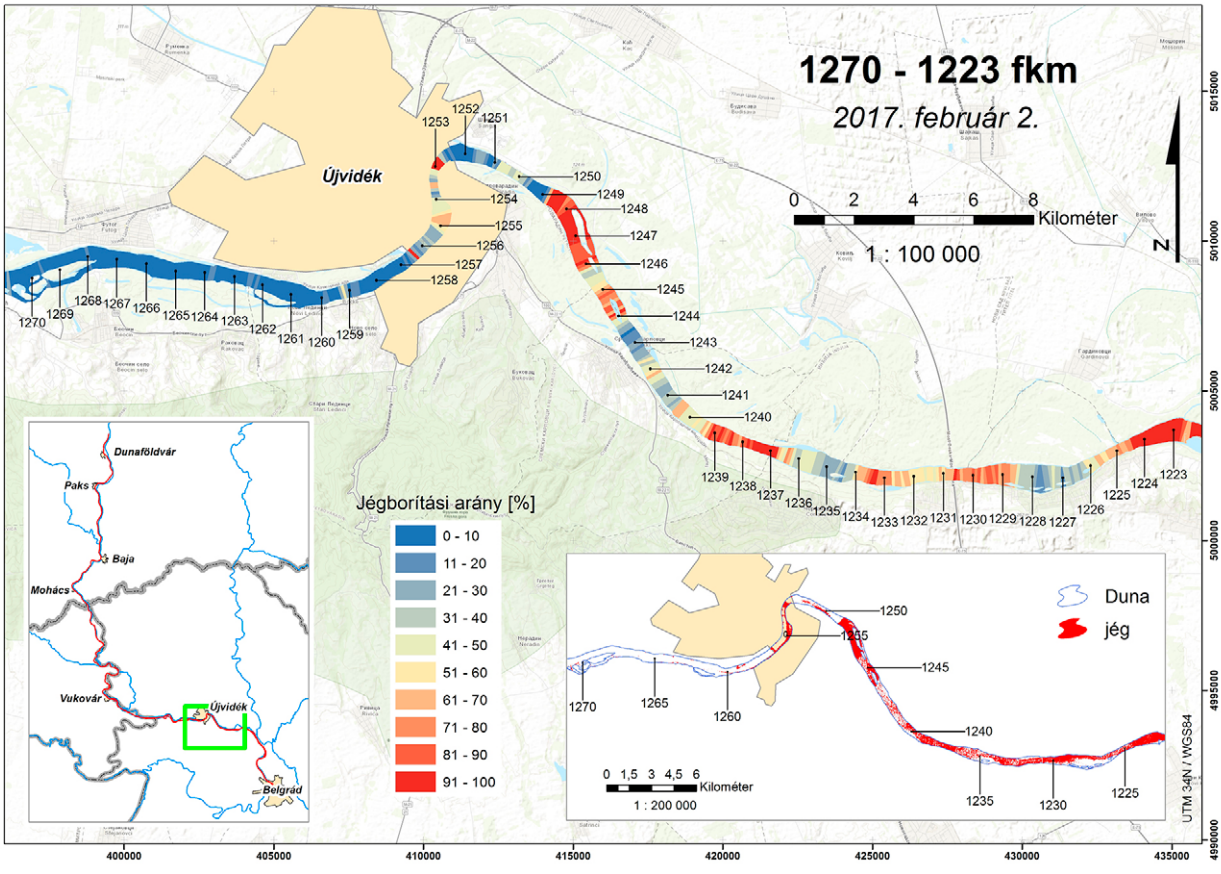


**Figure 7.** Sample layout of a selected Danube section (1270-1223 river km) on February 2, 2017

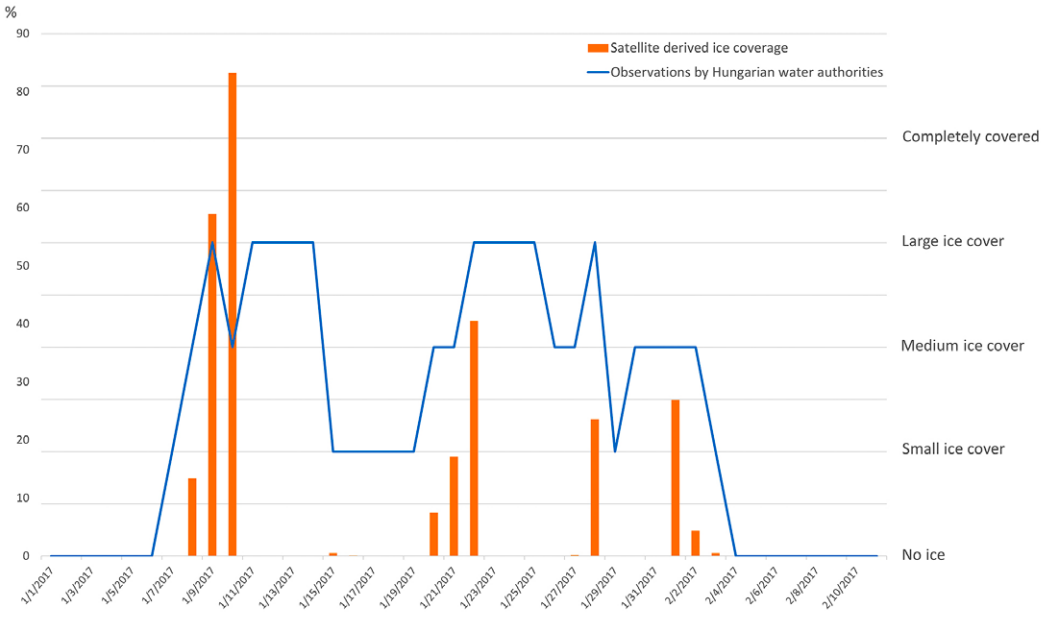


**Figure 8.** Comparison of satellite derived ice coverage in percentage and in situ observation by the Hungarian General Directorate of Water Management (https://www.hydroinfo.hu) for a section of the Danube between the cities of Dunaföldvár and Bölcske in 2017. Only dates when the satellite image was available are shown on the x -axis

terpretation of the amount of ice on the river as seen from the shore. There is some similarity to the patterns shown by the satellite derived ice cover, but it is not very strong. The large increase in ice coverage between the 8th and 10th of January can be clearly observed in both data sets. Also, the ice accretion on the 20th and 28th of January and the 1st of February seems to be detected in both data sets, but the limited number of observations by the satellite in the third week of January almost completely missed the small ice coverage observed during the in-situ observations.

In 2017, visual inspection of ice coverage on a Landsat 8 multispectral image clearly shows white-greyish areas at the East (left) bank of the river (Figure 9B), while ice coverage derived from a Sentinel-1 image of the same day shows ice on the same parts of the river (Figure 9C). It is not possible to quantify the correlation between the ice coverage, since the images are not from exactly the same time, but they clearly show the same pattern.

The amount of ice during the 2017 period on the Tisza near Szeged shows similarities between the two data sets as well (Figure 10A and B), although the spatial distribution is not as similar as in the validation period in 2017.

## Temporal development of ice cover

During the study period the most extensive relative ice cover was experienced on the 9th of January, when 41% (~7700 ha) of the total 405 km long river reach was covered by ice. Based on the previous ice cover data (3rd of January) and the temperature curve, this intensive ice cover developed only in about 2-3 days, primarily due to the extreme cold period starting from the 6th of January (Fig. 11). However, by this time floating ice could develop on the river, as the ra-

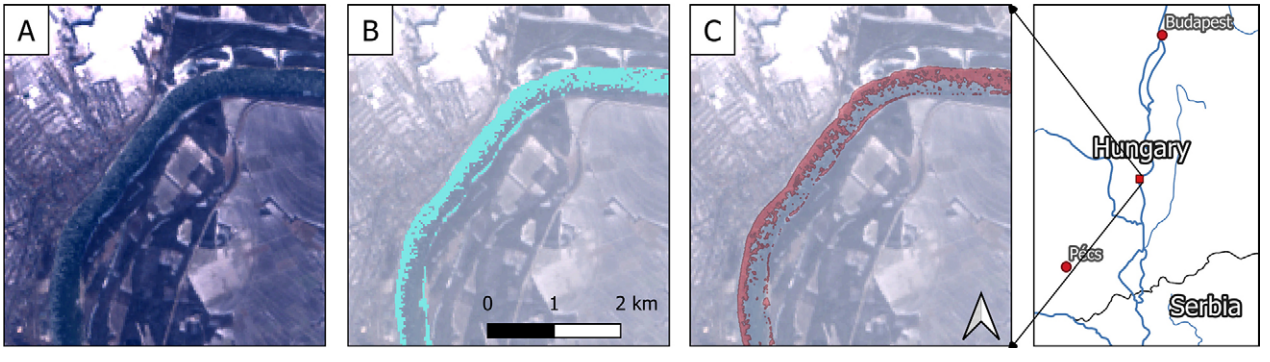


**Figure 9.** Validation of ice coverage derived from Sentinel-1 in 2017 on the Danube. Validation satellite image (Landsat 8 RGB432) (A), reference data derived by ISODATA clustering of Landsat 8 image (B), and ice coverage derived from Sentinel-1 satellite image (C). Sentinel-1 and Landsat 8 images were both acquired on January 22, 2017

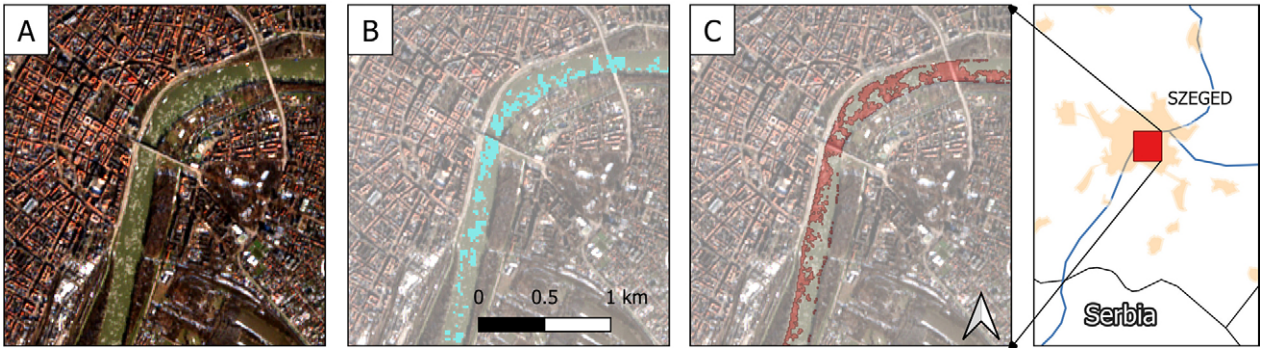


**Figure 10.** Validation of ice coverage derived from Sentinel-1 in 2022 on the Tisza. Validation satellite image (Sentinel-2 RGB843) (A), reference data derived by ISODATA clustering of Sentinel-2 image (B), and ice coverage derived from Sentinel-1 satellite image (C). Sentinel-1 and Sentinel-2 images were both acquired on January 24, 2022

tio of sections covered by static ice (ice cover ratio over 90%) was 1.1%. Although in the following days some warming was experienced, but daily means hardly reached 0°C, thus total ice cover did not increase, but the proportion of 100 m river polygons covered by static ice steadily increased (Fig. 11), even though, due to a short warming, the total ice cover decreased. In the next cold spell, the total ice cover remained 30-40 %. The maximum extension of static ice was experienced on the 28th of January. Total ice cover on the reach decreased by this time due to a slight warming (Fig. 11). This pattern refers to the pronounced formation of packed ice developing from an increased volume of ice floes on the river.

Due to a significant warming experienced from the beginning of February thawing advanced rapidly, ice cover halved in 2-3 days, and static ice cover dropped even more significantly.

## Spatial pattern of ice development

Based on the time averaged 100 m ice cover data for the entire period, three zones of increased ice formation and ice floe congestion can be identified on the investigated river section. The first ice formation zone (Zone I.) is located between Dunaföldvár and Paks. In this zone, the time averaged data reached a maximum of 40%, except for a short section right upstream of the road bridge over the river at Dunaföldvár (Fig. 12). As on each survey day and at each bridge, a significant ice cover was detected, it is assumed that at bridges the designed algorithm gives false positive results, which is also supported by the fact that the dielectric constant of ice (ε=3–4) is very close to that of asphalt (ε=4–5) as opposed to that of water (ε=80).

The second ice formation zone (Zone II.) is located between Apatin and Vukovar on a 70–80 km long section of the Danube, where time averaged ice cover values reached a maximum of 50% on a roughly 10 km long section (1355-1345 fkm). The third and most extensive section favouring ice formation and ice packing (Zone III.) is situated between Novi Sad and Belgrade (~90–100 km), where time averaged ice cover reached up to 60%.

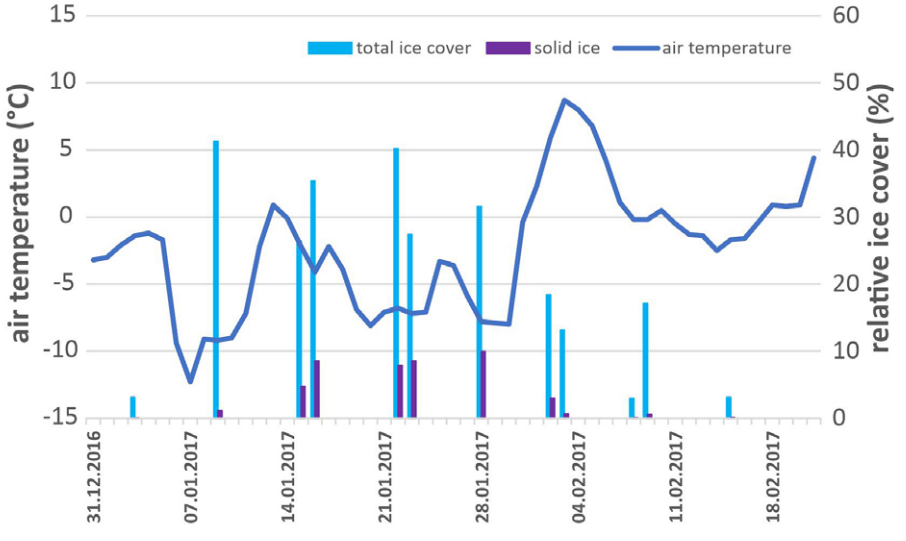


**Figure 11.** Daily mean air temperature between the period of 1st of January and 20th of February 2017, and the change of summed relative ice cover on the Dunaföldvár-Beograd section of the Danube River

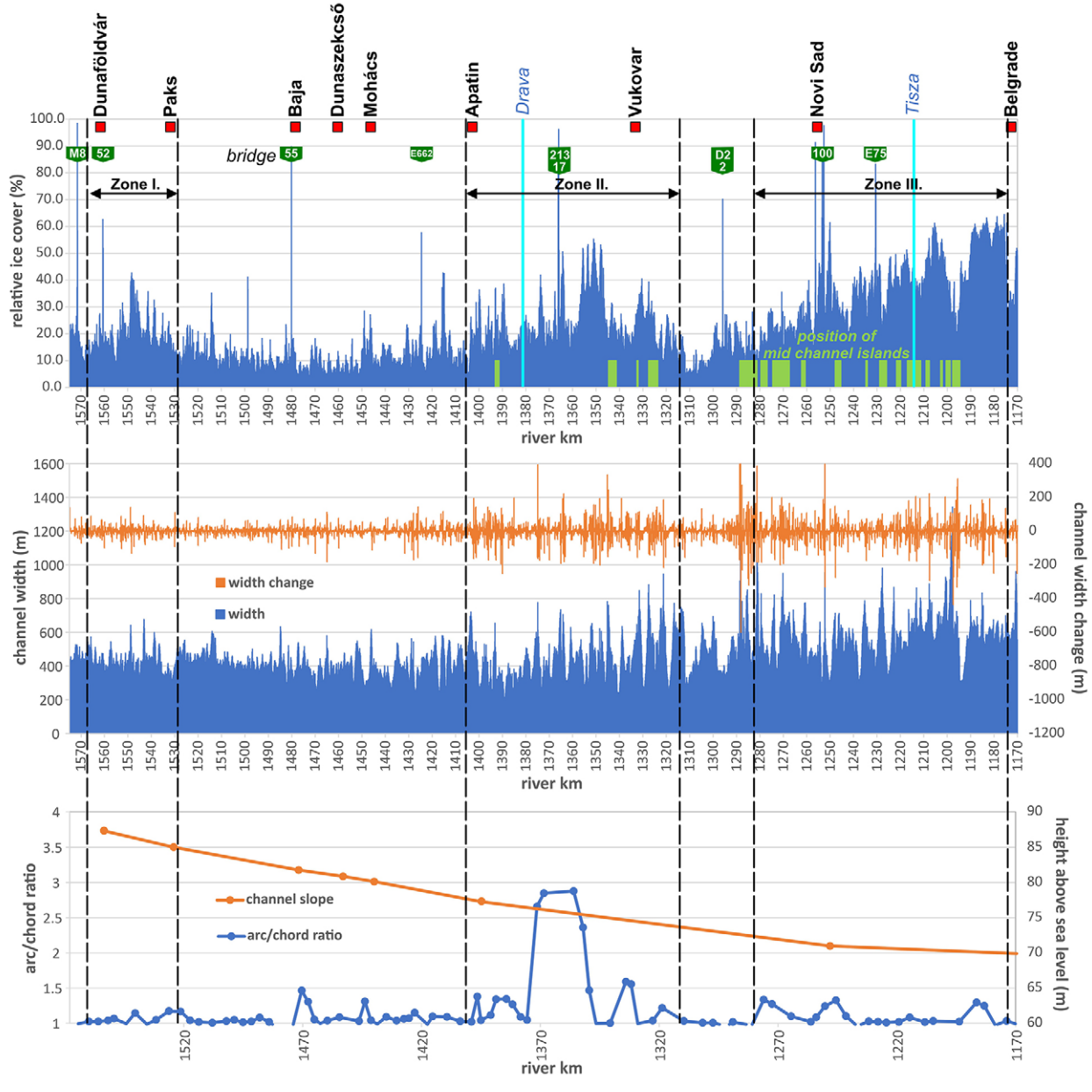


**Figure 12.** The time averaged distribution of ice cover on the investigated river reach, and the longitudinal change of channel geometric parameters (width, width change, meander arc/chord ratio, water surface slope at low water, position of islands)

The dynamics of ice transfer is also recognisable if the distribution of consecutive measurements is compared. On Figure 13, the survey made at the time of the largest ice cover (9th of January) is compared to the following surveys. It is clearly visible how floating ice moving from upstream is congested in the downstream ice zones, where full ice cover developed on several kilometre sections by this date, even though that day (15th of January) was right after the previously mentioned temporary warming (Fig. 11). On the next day (16th of January), as temperature decreased, ice formation, especially between Novi Sad and Belgrade, increased mostly because of local freezing. Ice transfer from upstream could have a secondary role in the increase of ice cover in the lack of time, as at an average velocity of the river (0.5 m/s) the transfer rate is 40-50 km/day. It must be also noted, that due to the temperature decrease, the ice formation started in ice zone I. as well (Fig. 13.).

## Spatial variation of channel geometry

The average width of the river on the investigated section is 464 m. Downstream of the confluence with the Drava and further on with the Tisza, two major tributaries of the Danube, the average channel width increases first by 88 m (from 406 to 494 m) then 136 m (from 494 to 615 m) (Fig. 12). The upstream part of the investigated section, till Apatin (1405 fkm) exhibits a

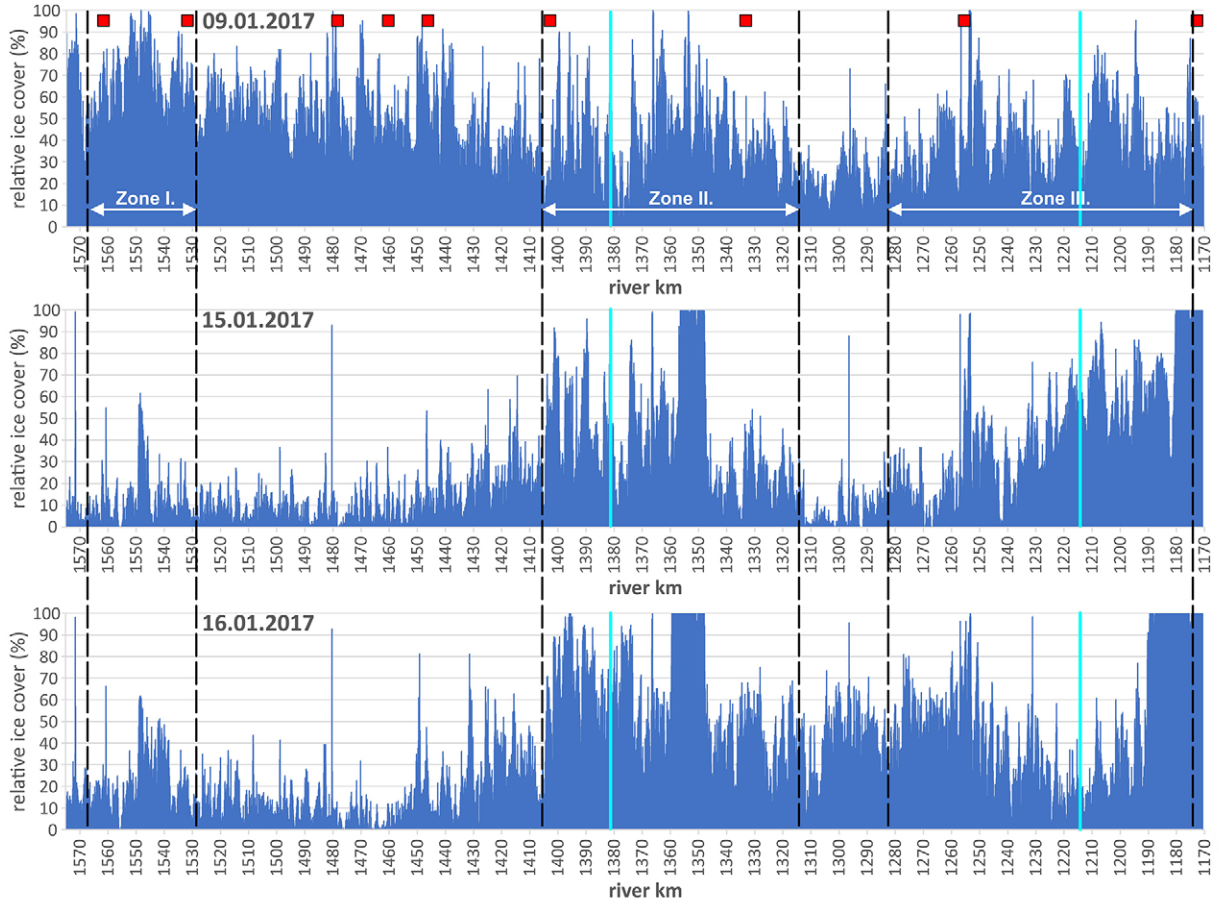


**Figure 13.** Changes in ice distribution on the study reach over three consecutive surveys. Red squares and cyan lines refer to the settlements and tributaries shown on Figure 12

lower variation in width values, being in average 19.5 m in absolute terms, equalling a roughly ±4.8% relative fluctuation. Going downstream, width variation increases, and a mean variation of 40 m can be observed, which even though the Danube gets wider corresponds to a ±8.4% mean fluctuation. However, there are longer sections, such as the one between 140 and 129 fkm, where fluctuation can reach a mean value of ±10% (Fig. 12).

An important feature affecting both width fluctuation and channel geometry in general is the presence of vegetated islands within the channel. In all 28 islands could be identified on the entire reach, most of them located on the lower section, between Vukovar and Belgrade. Their size shows a great variation; 13 out of them have a length below 1000 m, the rest are larger; their maximum length can reach 3000–4000 m.

Flow conditions are also affected by meanders and meander geometry. As the river has undergone significant regulations, the proportion of meandering sections is very limited. In total 91 river bends could be identified, but 70% of them is not a real bend (arc/chord length ratio < 1.1) (Fig. 12). The number of mature bends is only eight. Seven out of these are located between Apatin and Vukovar, which makes this the only meandering section of the study reach.

The mean slope of the river between Dunaföldvár and Belgrade (Pancevo) is 0.000044 m/m. Starting from 0.000079 m/m, between Dunaföldvár and Paks a generally decreasing trend can be seen in slope values in the downstream direction. The lowest value, 0.000014 m/m, was observed on the Novi Sad–Belgrade (Pancevo) section, which is under the impounding effect of the Iron Gate dam system (upper dam at 943 fkm).

## Discussion

The presented approach based on slicing of radar backscatter values into water and ice is a straightforward method that can be applied to large areas, with high resolution and with reasonable accuracy. The advantage of the approach is that the freely available satellite data is processed uniformly with an interval of about three days. The threshold between ice and water is determined empirically. The signal of ice is affected by its structure and water content. The strength of the signal of water is influenced by the turbulence in wa-

ter, caused by wind or other factors (Chu et al., 2015). All factors result in uncertainty of the threshold, but the validation results provide confidence that the determined threshold gives satisfying results.

River ice does not frequently occur in Hungary; During the last 6 years, we could only create satellite based maps for two ice periods. In the latest period, it was only possible to detect ice on the Tisza River and not on the Danube. Climate change models predict an overall rise of temperature for the Carpathian basin, but also more extreme weather patterns, and periods with extreme cold are likely to occur more often (Mezősi et al., 2016). Remote sensing techniques provide a cost effective solution to monitor river ice and provide operational information to the authorities for mitigation of damage due to ice dams and floods.

Beside the potential for development of a basin wide monitoring activity and decision support system, the satellite based survey made during the 2017 ice event also allows to draw some general conclusions in terms of ice formation and congestion on the study reach.

Not surprisingly, based on the obtained data series, slope is among the most important determinants of ice development, since decreasing slope showed an extension of ice formation zones (Fig. 12). This is because lower velocity enables more effective freezing and also the congestion of ice floes. Due to the continuous downstream increase of width, parallel to the decrease of slope, a slight positive correlation can be observed between width and relative ice cover if the entire period and the entire section is considered (Fig. 14). However, if sectors, having similar but variable width all along, e.g. the one between 1315 and 1405 fkm (Zone II.) are analysed, then such a relationship cannot be observed (Fig. 14). This is partly because both narrowing (by congestion) and widening (by slower velocity) can contribute to ice cover development.

Considering the identified three ice formation zones, high relative ice cover ratios are the result of the interplay of several factors. In case of Zone I., ice jams and static ice cover could appear regularly because of two mild bends (arc/chord ratio < 1.5), which exhibit a slightly higher width variation than upstream. It must be noted that in a downstream direction more mature bends are situated, still, at a lower

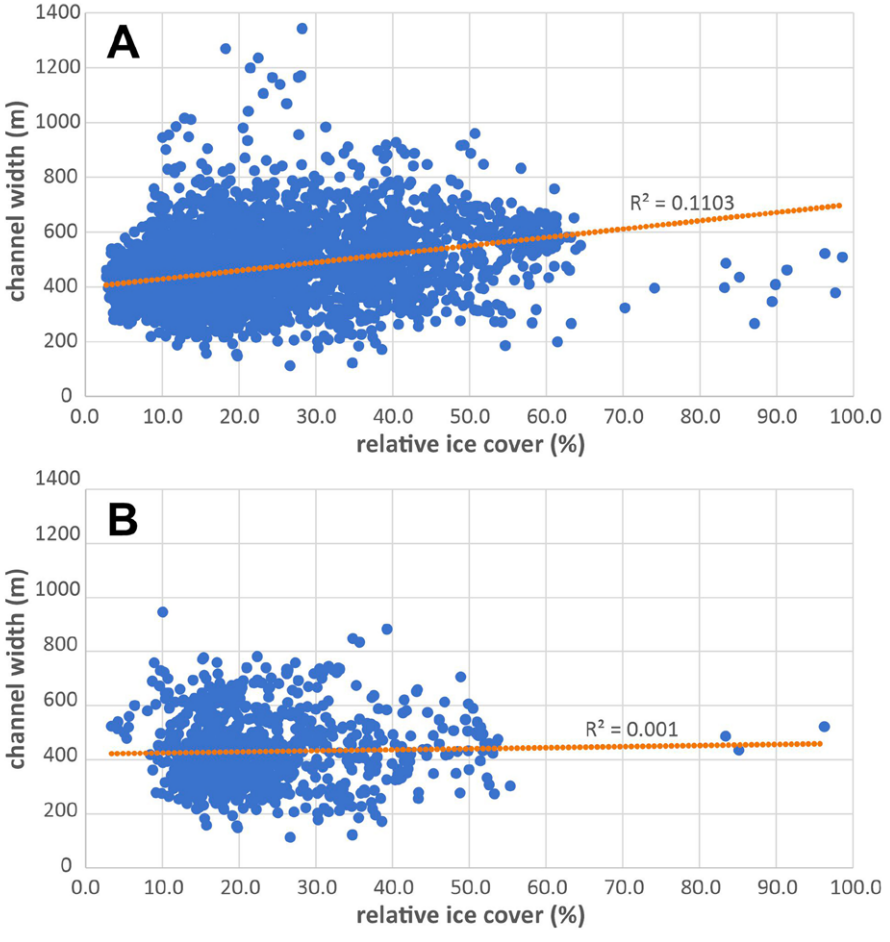


**Figure 14.** The relationship of width and ice cover A) on the entire study reach and B) on the reach of Zone II. with highly variable width conditions

width variation complete ice cover developed only in the coldest period.

Zone II. is the only true meandering section of the study area, besides, channel width variation is also significant here, and four mid channel islands obstruct the flow (Fig. 12). The formation of ice jams can clearly be related to four-five suddenly narrowing sections usually located at the apex of meanders, or at the confluence of anabranches at the downstream end of islands. Consequently, this was one of the sections where ice breaker ships had to intervene to avoid impoundment caused by piled up ice floes (Babic Mladenovic et al., 2017).

In accordance with Babic Mladenovic et al, (2017), the largest scale static ice formation occurred in Zone III., at Novi Sad and Belgrade. Here the most important drivers of static ice development were the backwater effect of the Iron Gate Dam I. and the resulting decrease of water surface slope and flow velocity (Fig. 12). However, based on Serbian ice cover reports, ice development downstream of Belgrade was less critical (Babic Mladenocic et al., 2017), which underlines the role of large tributaries, since the Sava River joining the Danube at Belgrade was not carrying much ice, whereas the Tisza, having its confluence in this zone, was heavily frozen. However, the impact of channel geometry must also be underlined in case of Zone III., since for example the significant narrowing at 1196 fkm, accompanied with the presence of some larger bends and mid-channel islands made the area ideal for the development of ice jams (Fig. 12).

## Conclusion

Continuous monitoring of river ice is important not only for preventing and reducing floods, but also to prevent and decrease the impact of damage in river infrastructure. The presented method is a cost effective, remote sensing-based approach that can provide operational maps over large areas at high spatial (10 m) and relatively high temporal (2-3 days) resolution. The dataset complemented with field observations can aid interventions and support operational decision making.

Although the quantitative validation of ice cover detection results is problematic, the comparison with in-situ observations and other optical satellite data sets shows good comparability. Field observations are subjective, as they can mostly be made from the river bank. The radar-based ice coverage algorithm is objective and uniform over the total length of rivers. The algorithm is automated, provides robust results as long as Sentinel-1 data is available and can be applied in other regions as well. The application of other data sources, like IP cameras for continuous monitoring would help to refine and calibrate our satellite-based ice observation method.

The spatial and temporal evolution of ice coverage is very important for forecasting and analysing ice flow processes. Based on the 2017 data, the interplay of various parameters determines the location of ice jam development on the study reach. Among all, flow velocity, primarily governed by water surface slope, determines at most the intensity of ice accumulation and static ice cover formation. However, the role of channel geometry is also important, as increased channel width variability, high sinuosity or the presence of mid-channel islands are key parameters in the development of ice jams. The severity of the ice event is also greatly determined by the amount of ice arriving on the tributaries.

The present survey has also shown the dynamic character of ice formation and ice congestion. The appearance of ice floes on the upstream sections was quickly followed by the formation of packed ice on geometrically variable or low slope sections downstream. The data obtained in this study can help engineers to better identify critical cross-sections where preventive interventions are needed to better manage ice events in the future.

## Acknowledgements

*We are grateful for the General Directorate of Water Management of Hungary for their support of the research.*

## References

Agafonova, S., Frolova, N., Krylenko, I., Sazonov, A., & Golovlyov, P. (2017). Dangerous ice phenomena on the lowland rivers of European Russia. *Natural Hazards*, 88. http://dx.doi.org/10.1007/s11069-016-2580-x.

Altena, B., & Kääb, A. (2021). Quantifying river ice movement through a combination of European satellite monitoring services. *International Journal of Applied Earth Observation and Geoinformation*, 98, 102315, http://dx.doi.org/10.1016/j.jag.2021.102315

Babić Mladenović, M., Gombás, K., Liška, I., & Balatonyi L. (2017). Report on the ice event 2017 in the Danube River Basin. ICPDR-IKSD. available at: https://www.icpdr.org/main/sites/default/files/nodes/documents/report_ice_event_2017_0.pdf

Chu, T., Das, A., & Lindenschmidt K-E. (2015). Monitoring the variation in Ice-Cover Characteristics of the Slave River, Canada using Radarsat-2 data – A case study. *Remote Sensing*, 7, 13664-13691. https://doi.org/10.3390/rs71013664

Gombás K., & Balatonyi L. (2017). Extremities in winter season - outlook for mitigation measures. *Hidrológiai Közlöny*, 97(3), 81-85. available at: https://adt.arcanum.com/hu/view/HidrologiaiKozlony_2017/?pg=0&layout=s

Goldberg, M.D., Li, S., Lindsey, D.T., Sjoberg, W., Zhou, L., & Sun, D. (2020) Mapping, Monitoring, and Prediction of Floods Due to Ice Jam and Snowmelt with Operational Weather Satellites. *Remote Sensing*, 12(11), 1865. https://doi.org/10.3390/rs12111865

Hicks, F. (2009). An overview of river ice problems: CRIPE07 guest editorial. Cold Regions Science and Technology, 55, 175-185. http://dx.doi.org/10.1016%2Fj.coldregions.2008.09.006

Horváth, Á. (2017), 2017 jeges januárja [2017 ici january]. *OMSZ Tanulmányok*, http://www.met.hu/ismeret-tar/erdekessegek_tanulmanyok/index.php?id=1805&hir=2017_jeges_januarja

Howell, S.E.L., Brady, M., & Komarov, A.S. (2021). Large-scale sea ice motion from Sentinel-1 and the RADARSAT Constellation Mission. The *Cryosphere Discuss.*, https://doi.org/10.5194/tc-2021-223 (Preprint)

Ionita, M., Badaluta, C.A., Scholz, P., & Chelcea S. (2018). Vanishing river ice cover in the lower part of the Danube basin – signs of a changing climate. *Scientific Reports*, 8, 7948. https://doi.org/10.1038/s41598-018-26357-w

Keve, G. (2014). Jégészlelés a Duna magyarországi alsó szakaszán [Ice detection on the lower section of the Danube in Hungary]. Magyar Hidrológiai Társaság XXXII. Országos Vándorgyűlés. Szeged, Hungary, July 2-4,2014. Budapest: Magyar Hidrológiai Társaság (MHT), pp. 19

Keve, G. (2017a). Utilization of gained experiences based on ice observation by webcameras. XXVII Conference of the Danubian Countries on Hydrological Forecasting and Hydrological Bases of Water Management, Bulgaria. 68-78.

Keve, G. (2017b). Space-time ice monitoring of the Hungarian Lower-Danube. *Periodica Polytechnica-Civil Engineering*, 61(1). 27-38. https://doi.org/10.3311/PPci.9116

Keve, G. (2020). Determining accurate ice coverage on Danube by webcameras. In: *Proceedings of XXVII Conference of the Danubian Countries on Hydrological Forecasting and Hydrological Bases of Water Management,* https://doi.org/10.15407/uhmi.conference.01.03.

Kiss, T., Fiala, K., Sipos, Gy., & Szatmári, G. (2019). Long-term hydrological changes after various river regulation measures: are we responsible for flow extremes? *Hydrology Research*, 50(2), 417–430. https://doi.org/10.2166/nh.2019.095

Lal, A. W., & Shen, H. T. (1993). A mathematical model for river ice processes. *Journal of Hydraulic Engineering*, 117(7). http://dx.doi.org/10.1061/(ASCE)0733-9429(1991)117:7(851)

Li, X. -M., Sun, Y., & Zhang, Q. (2021) Extraction of Sea Ice Cover by Sentinel-1 SAR Based on Support Vector Machine With Unsupervised Generation of Training Data. *IEEE Transactions on Geoscience and Remote Sensing*, 59(4), 3040-3053, https://doi.org/10.1109/TGRS.2020.3007789

Liptay, Z., Czigány, Sz., & Pirkhoffer, E. (2021). River ice and water temperature prediction on the Danube. *Hungarian Geographical Bulletin*, 70, 201-214. https://doi.org/10.15201/hungeobull.70.3.1.

Lohse, J., Doulgeris, A., & Dierking, W. (2020). Mapping sea-ice types from Sentinel-1 considering the surface-type dependent effect of incidence angle. *Annals of Glaciology*, 61(83), 260-270. https://doi.org/10.1017/aog.2020.45

Malenovský, Z. Rott, H. Cihlar, J. Schaepman, M.E. García-Santos, G. Fernandes, R., & Berger, M. (2012). Sentinels for science: Potential of Sentinel-1, -2, and -3 missions for scientific observations of ocean, cryosphere, and land, *Remote Sensing of Environment*, 120, 91–101, https://doi.org/10.1016/j.rse.2011.09.026

Mezősi, G. (2016). *The physical geography of Hungary.* Springer International Publishing.

Mezősi, G. Blanka, V. Bata, T. Ladányi, Zs. Kemény, K., & Meyer, B.C. (2016). Assessment of future sce-

narios for wind erosion sensitivity changes based on ALADIN and REMO regional climate model simulation data. *Open Geosciences*, 8(1), 465-477. https://doi.org/10.1515/geo-2016-0033

OMSZ, Elmúlt évek időjárása (Weather in past years ), 2017. https://www.met.hu/eghajlat/magyarorszag_eghajlata/eghajlati_visszatekinto/elmult_evek_idojarasa/

Somogyi, S. (2001). Természeti és társadalmi hatások a Duna mai vízrendszerében (Natural and social impacts in catchment of Danube). *Hungarian Geographical Bulletin/Földrajzi Értesítő*, 50(1-4), 299-310.

Takács, K., & Kern, Z. (2017): Long-term ice phenology records of Lake Balaton and the Danube River (East Central Europe). PANGAEA, *https://doi.org/10.1594/PANGAEA.881056*

Takács, K., Kern, Z. & Pásztor, L. (2018). Long-term ice phenology records from eastern–central Europe, *Earth System Science Data*, 10, 391–404, https://doi.org/10.5194/essd-10-391-2018

Tom, M., Aguilar,R., Imhof, P., Leinss, S., Baltsavias, E., & Schindler, K. (2020) Lake ice detection from Sentinel-1 SAR with deep learning, arXiv:2002.07040v2 [eess.IV]

Unterschultz, K.D., van der Sanden, J., & Hicks, F.E., (2009). Potential of RADARSAT-1 for the monitoring of river ice: Results of a case study on the Athabasca River at Fort McMurray, Canada, *Cold Regions Science and Technology*, 55(2), 238-248, https://doi.org/10.1016/j.coldregions.2008.02.003

Van Leeuwen, B., & Tobak, Z. (2018). Satellite data based river ice monitoring, In: Molnár, V. (Ed.), Az elmélet és a gyakorlat találkozása a térinformatikában IX.: Theory meets practice in GIS Conference, Debrecen, Hungary, Debreceni Egyetemi Kiadó. pp. 371-376. ISBN 978-963-318-723-4

Weber, F., Nixon, D., & Hurley, J. (2003). Semi-automated classification of river ice types on the Peace River using RADARSAT-1 synthetic aperture radar (SAR) imagery. *Canadian Journal of Civil Engineering*, 30, 11–27, https://doi.org/10.1139/l02-073

Zakharova, E., Agafonova, S., Duguay, C., Frolova, N., & Kouraev, A. (2021). River ice phenology and thickness from satellite altimetry: potential for ice bridge road operation and climate studies. *The Cryosphere*, 15, 5387-5407. https://doi.org/10.5194/tc-15-5387-2021

Zhang, Y., Zhu, T., Spreen, G., Melsheimer, C., Huntemann, M., Hughes, N., Zhang, S., & Li, F. (2021). Sea ice and water classification on dual-polarized Sentinel-1 imagery during melting season. *The Cryosphere Discuss.*, https://doi.org/10.5194/tc-2021-85 (Preprint)